Cluster Approach for Quasicrystals

Hyeong-Chai Jeong and Paul J. Steinhardt
Department of Physics, University of Pennsylvania, Philadelphia, Pennsylvania 19104
(Received 8 April 1994)

We consider a "cluster picture" to explain the structure and formation of quasicrystals. Quasicrystal ordering is attributed to a small set of low-energy atomic clusters which determine the state of minimum free energy. The nature of the ground state as $T \to 0$, depending upon the clusters and cluster energies, ranges from energetically stable and unique (as in Penrose tilings), to entropically stable and degenerate (as in random tilings).

PACS numbers: 61.44.+p, 05.50.+q, 61.50.Ks

Since the discovery of the first icosahedral alloy [1], a fundamental question has been: Why do quasicrystals form? In this Letter, we explore a "cluster picture" based on the concept that the structure of a solid can be determined by the lowest-energy atomic clusters. The low-energy clusters are responsible for making the quasicrystal the state of minimum free energy. The idea is similar to a notion commonly invoked to explain periodic crystals: macroscopic crystal structure results from periodic, dense-packing of some microscopic, low-energy cluster. There is numerical evidence that low energy clusters can form in the melt and join together during solidification to form ordered structures [2]. In its application to quasicrystals, an important element is that the low-energy clusters can overlap to further increase their density. That is, an atom can participate in two or more distinct low-energy clusters. Energy minimization favors cluster overlap and, we conjecture, a network of overlapping clusters can induce strong correlations between distant regions that enhances quasiperiodic ordering. Clusters have been noted previously as important elements in specific atomic models of quasicrystals [3–7]; there is evidence of a hierarchy of cluster structures, e.g., in icosahedral AlPdMn [8]; and, recently, clusters have been invoked to explain the electronic resistivity and diamagnetic properties [9]. In this paper, clusters take center stage as the generic, primary influence promoting quasicrystal formation. Together with the previous work, a significant implication is that the focus should be on the energetics of microscopic atomic clusters in order to explain macroscopic quasiperiodic ordering or to predict new quasicrystalline alloys.

The nature of the ground state in the cluster picture depends on the specific choice of clusters and energies. The ground state as $T \to 0$ can range from energetically stable and unique, as in Penrose tilings [10,11], to energetically stable and degenerate, as in tilings with "weak" matching rules [12], to entropically stable, as in random [3,13] tilings. This leads us to reinterpret prior, competing tiling models of quasicrystals as part of a spectrum of cluster picture possibilities. In this approach, no single prior model is preferable overall; rather, the best-fitting model for any real quasicrystal depends on the low energy clusters for the particular elemental composition. In this sense, the cluster picture might serve as a unifying theoretical approach that spans all quasicrystal solids.

Our analysis is based on numerical studies of 2D and 3D tilings. The different types of tiles represent different atoms or groups of atoms which close-pack to form the solid. In this paper, we focus on 2D models with decagonal symmetry constructed from fat (f) and skinny (s) rhombus tiles (see Fig. 1), which is relevant for describing the periodically spaced layers of 3D decagonal quasicrystals. The cluster picture entails selecting a small set of tile clusters, $\{i\}$, which are assigned an energy per cluster $\epsilon_i < 0$. All other clusters are assigned $\epsilon = 0$. The free energy is minimized using this chosen Hamiltonian.

For the free-energy minimization, we use conventional Metropolis Monte Carlo methods used in our studies of elastic phase transitions [14] and recent entropic sampling Monte Carlo techniques [15]. All close-packed tile configurations are checked for a sequence of periodic approximants to the quasicrystal. The stoichiometry can be defined in terms of the fractional area occupied by fat tiles, $x = (\tau N_f)/(\tau N_f + N_s)$, where $N_{(f,s)}$ is the number density of (fat, skinny) tiles and $\tau \equiv (1 + \sqrt{5})/2$ (the golden ratio). The quasicrystal has $x = x_0 \equiv \tau^2/(\tau^2 + 1)$ and a periodic approximant has x equal to some rational approximant to x_0. We consider two sequences of periodic approximants which approach $x = x_0$ from

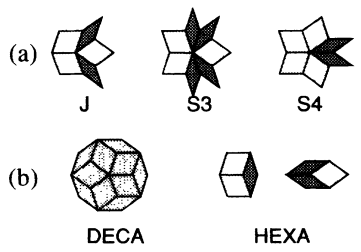

FIG. 1. Low-energy clusters selected for the examples in this paper: (a) C_P: J, $S3$, and $S4$; C_W: J and $S3$. (b) $C_{B/T}$: Decagon clusters (only the "star" decagon cluster is shown here, but there are five others) and the two hexagon clusters. C_D: star decagon cluster only.

0031-9007/94/73(14)/1943(4)$06.00

above and below: fat-tile-shaped approximants with $x = (F_{2k+1} + F_{2k-1})/(\tau^{2k} + \tau^{2k-2}) > x_0$ (where F_k is the kth Fibonacci number) and skinny-tile-shaped approximants with $x = (F_{2k} + F_{2k-2})/(\tau^{2k-1} + \tau^{2k-3}) < x_0$. Minimizing the free energy for both sequences allows us to study the stability of the quasicrystal phase as a function of stoichiometry. Although there are strong indications that our simulations converge on the true, thermodynamic ground state, our conclusions should be regarded as numerical and not rigorously proven.

The limit in which $\epsilon_i = 0$ for all clusters is a realization of the "maximally random" tiling model [3,13]. Every close-packed configuration has equal internal energy independent of stoichiometry, x. For fixed x, the number of degenerate configurations of a system of total area A grows as $\exp(\sigma A)$, where σ is the entropy per unit area. According to the random tiling hypothesis [13,16] configurations with quasicrystalline order (and $x = x_0$) have the highest σ. Hence, for $T > 0$, the quasicrystal is the state of lowest free energy. The maximal random tiling is a good approximation for quasicrystals at high T when the thermal energy exceeds all internal energies. Here, however, we are interested in behavior at moderate to small T. In this case, the maximally random tiling condition that all close-packed arrangements of tiles have equal energy seems unlikely to apply to real quasicrystals where atomic clusters replace the tiles.

The cluster picture is motivated by the more likely condition that some clusters have lower energy than others. This breaks the energy degeneracy and, depending on the clusters and cluster energies, can lead to ground states ranging from Penrose-tiling-like to random-tiling-like at $T = 0$. Below, we illustrate the spectrum of possibilities using four 2D examples. Because of properties special to two dimensions, the distinctions are somewhat blurred for $T > 0$; namely, thermal fluctuations result in a transformation of a 2D Penrose tiling at $T = 0$ to random tiling elastic behavior and degeneracy at $T > 0$ [13,17]. However, it is useful to make these distinctions anyway to understand quantitative differences (e.g., in elastic constants) as $T \to 0$ in two dimensions. More importantly, 2D is a testing ground for three dimensions, where the different $T = 0$ phases should remain stable for a finite range of $T > 0$ [14]. With this caveat, we first consider the ground states as $T \to 0$ for fixed stoichiometry, $x = x_0$.

C_P (*Penrose-like*).—At $T = 0$, the ground state is unique. Our example was designed to obtain a perfect Penrose tiling [11], although it seems possible to obtain other unique ground states. There are three low energy clusters labeled $S3$, $S4$, and J [using de Bruijn's notation [18], see Fig. 1(a)]. We assign cluster energies $\epsilon_{S4} \approx \epsilon_J \approx -1$ and $\epsilon_{S3} \approx -2$, and $\epsilon = 0$ for all other clusters. As in all of our examples, the ground state does not depend sensitively (e.g., $\pm 50\%$) on the absolute or relative energies. Even though the ground state is the same, this cluster picture model is different from the "matching rule" picture [10] based on Penrose tiling. The Penrose tiling is uniquely forced by a set of "matching rules" which specify the way *every* pair of tiles join together edge-to-edge [11]. The matching rules can be translated into an extreme limit of cluster rules in which one identifies *all* local arrangements of tiles (out to some finite distance) as being low-energy clusters. For example, the matching rules can be recast as the condition that all seven clusters that appear in Penrose tiling have $\epsilon = -1$ and all others have $\epsilon = 0$. In contrast, example C_P specifies only three cluster configurations. The three clusters were consciously chosen so as to bias the s-tile environments to be Penrose-like. However, it is cluster overlap (induced by energy minimization) along with geometric and close-packing constraints which, in a nontrivial way, uniquely fix the local arrangements in the structure at $T = 0$.

C_W (*weak-matching-rule-like* [12]).—The cluster choice is the same as C_P except $\epsilon_{S4} \to 0$. Unlike C_P, the ground state is degenerate, and there is finite entropy per tile (σ). The Penrose tiling is among the degenerate ground states, but one can also rearrange certain isolated islands of tiles to obtain new configurations of equal energy. Since the differences entail only isolated islands of tiles, all ground state configurations exhibit long-range quasiperiodic order as Penrose tiling. Tilings with weak matching rules [12] have similar characteristics.

$C_{B/T}$ (*random-binary– or two-level–tiling-like*).—For x near x_0, the ground state is degenerate such that each ground-state configuration can be resolved into a decoration of random-binary or two-level tilings [3], two distinct types of modified random tilings with matching rules which limit the vertex types. By decoration, we mean that each tile type in a binary or two-level tiling is replaced by some specific cluster of f and s tiles. For example, if we assign $\epsilon_D = -1$ to all decagonal configurations of five f and five s tiles and $\epsilon_H = -\delta$ to the two hexagon configurations shown in Fig. 1(b) where $0 < \delta \ll 1$, we obtain a decoration of the binary tiling shown in Fig. 2.

C_D (*discrete ordered*).—Generically, we find that cluster models display "discrete order" (defined below); we classify as C_D models which exhibit discrete order but do not obey Penrose, weak, or binary/two-level matching rules. (N.B. The maximally random tiling is *not* discrete-ordered.) An example is obtained by assigning low energy only to the star decagon [Fig. 1(b)]. For both cases with degenerate ground states, $C_{B/T}$ and C_D, the energy varies linearly with x at $T = 0$ so that the quasicrystal ($x = x_0$) is unstable (see below). However, if the random tiling hypothesis applies, the quasicrystal is entropically stabilized at finite T.

To quantify the long-range order, we compute the "perp-space images" [19,20]: Each 2D tiling vertex can be expressed as $\sum_i n_i \mathbf{e}_i^{\parallel}$, where n_i is an integer and $\mathbf{e}_i^{\parallel} = (\cos[2\pi i/5], \sin[2\pi i/5])$. The perp-space image is the

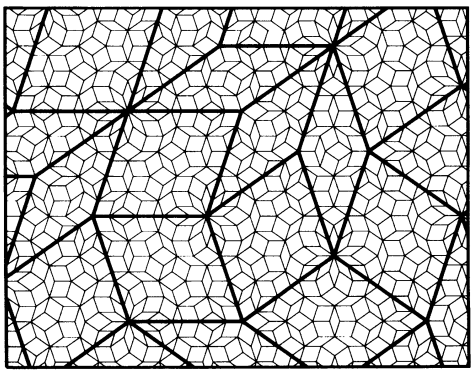

FIG. 2. A sample ground state configuration for $C_{B/T}$ obtained for low energy clusters shown in Fig. 1(b). The configuration is a decoration of a binary tiling (shown in heavy outline). The binary matching rule constrains tile edges joining at any given vertex to be separated by angles that are either even or odd multiples of $2\pi/10$.

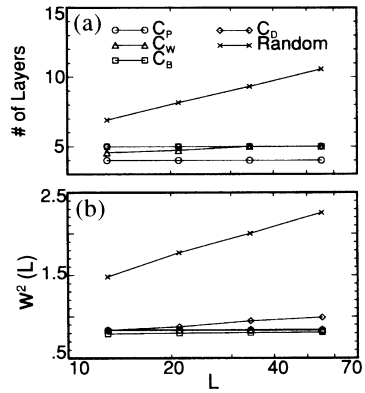

FIG. 3. Plots illustrating (a) the distribution in d_N (discrete order); (b) the mean-square phason fluctuations, $w^2(L)$, as a function of tiling size, illustrating phason disorder in maximally random tilings compared to cluster picture examples.

3D set of points obtained by mapping each vertex into $\mathbf{v}_n = \sum_i n_i \mathbf{e}_i^{\perp}$ where n labels the tiling vertex and $\mathbf{e}_i^{\perp} = (\sqrt{2/5}\cos[4\pi i/5], \sqrt{2/5}\sin[4\pi i/5], \sqrt{1/5})$. $\mathbf{v}_n$ can be resolved into a z-component d_n (equal to an integer times $1/\sqrt{5}$) which takes on discrete values and continuous x-y components $\mathbf{w}_n$, known as the phason variables. The translational order is characterized by the correlations in d_n ("discrete ordering") and $\mathbf{w}_n$ ("phason ordering").

All four cluster picture examples are "discrete ordered" in the sense that the mean-square fluctuation in d_n, $d^2(L)$, remains finite as $L \to \infty$. We define $d^2(L) = \langle \frac{1}{N} \sum (d_n - \bar{d})^2 \rangle$, where N is the number of vertices, $\bar{d} \equiv \frac{1}{N} \sum d_n$, and $\langle \cdots \rangle$ represents the ensemble average. In fact, as shown in Fig. 3(a), d_n is completely confined to four or five values, depending on the example. We have been able to construct examples which are not discrete ordered, but this is not typical if there is cluster overlap. This constrasts with the maximally random tiling, for which the d_n spreads over infinitely many values and $d^2(L)$ diverges logarithmically with system size. Figure 3(b) shows the mean-square phason fluctuations at $T = 0$, $w^2(L) = \langle \frac{1}{N} \sum (\mathbf{w}_n - \bar{\mathbf{w}})^2 \rangle$, where $\bar{w} = \frac{1}{N} \sum \mathbf{w}_n$. In the three cases with degenerate ground states (maximal random tiling, C_D, and $C_{B/T}$), $w^2(L)$ diverges logarithmically with L. [$d\, w^2(L)/d \ln L$ is so small for $C_{B/T}$ that the divergence is not discernible in the figure.] A consequence is that, for these cases, the ground state exhibits power-law (rather than Bragg) diffraction peaks and that there is a diffuse scattering background [21]. However, the fact that the slope, $d\, w^2(L)/d \ln L$, is so much smaller for the cluster models means that the diffuse scattering is much less for the cluster models compared to the random tiling pictures. C_P and C_W exhibit long-range phason order; the diffraction patterns for both exhibit Bragg peaks. For C_W, there is also disorder due to the freedom to flip tiles within isolated islands, which results in some very small diffuse background. Altogether, it seems that the cluster picture produces dramatically reduced or zero diffuse scattering. This is notable since some highly ordered quasicrystal solids observed in the laboratory fail to exhibit measurable diffuse scattering.

The slope in Fig. 3(b) is also a measure of the phason-phason elastic constant as $T \to 0$. The reader is reminded that quasicrystals exhibit both phonon and phason elastic modes [22]. If the structure is described as a sum of mass density waves, phonon modes are related to overall translations and phason modes are related to relative translations of incommensurate density waves. In a tiling picture, phasons correspond to tile rearrangements. Phason strain is defined as $e_{ij} = \partial_j w_i$, where $\mathbf{w}$ is the phason field (a coarse-grain average of $\mathbf{w}_n$ defined above). In cases where the phason elastic energy, $\mathcal{E}$, is quadratic in the phason strain [3,13] (sometimes referred to as "unlocked" phason elasticity), $\mathcal{E} = \frac{1}{2}\kappa_1 \sum_{ij} e_{ij} e_{ij}$, where the phason-phason elastic constant can be obtained from the mean-square phason fluctuations according to $\kappa_1 \sim T(\pi\, d\, w^2(L)/d \ln L)^{-1}$. Table I indicates the value of κ_1/T as $T \to 0$. Note that, formally, κ_1/T is divergent for C_P and C_W; this is an indication that the phason elastic energy is linear, rather than quadratic, in the phason strain at $T = 0$ (sometimes called "locked" phason elasticity), $\mathcal{E} \propto |e_{ij}|$. Whether the phasons are locked or unlocked, the general trend is that the effective phason-phason elastic constant is significantly larger for cluster models compared to random tilings.

We have also studied the stability of quasicrystals at $T = 0$ as a function of stoichiometry, x, by evaluating the internal energy $\mathcal{U}(x)$ for a sequence of periodic approximants with $\Delta x = x - x_0 \neq 0$. We find that $\mathcal{U}(x)$ can be fit to the form: $\mathcal{U}(x) = \alpha_1 x + \alpha_2 |\Delta x|^{\frac{1}{2}}$. For C_W, we find that we must fit separately $\Delta x > 0$ and $\Delta x < 0$. See Table I. [This form was motivated by considering

TABLE I. Comparison of 2D cluster picture and random tiling models.

Model	Stability	κ_1/T	α_1	α_2
C_P	Energetic	∞	0.447	0.33
C_W	Energetic	∞	5.407	0.33 for $\Delta x < 0$ 0 for $\Delta x > 0$
$C_{B/T}$	Entropic	30.5	−3.789	0.
C_D	Entropic	3.56	0.324	0.
Max random	Entropic	0.60	0.	0.
Binary	Entropic	0.62	0.	0.

how the elastic energy $\mathcal{E}$ varies with uniform phason strains at $T = 0$. A uniform phason strain produces a shift in x such that $\mathcal{E}(x) \propto x$ in the unlocked phase and $\mathcal{E}(x) \propto |\Delta x|^{\frac{1}{2}}$ in the locked phase [3].] For C_P and C_W, we find a stable minimum at $\Delta x = 0$ which is cusplike; hence, there is an energetically stable quasicrystal phase at $T = 0$ [23]. For $C_{B/T}$ and C_D, $\alpha_2 = 0$ and $\mathcal{E}(x)$ varies linearly with x. The quasicrystal ($\Delta x = 0$) is unstable at $T = 0$, but, if the random tiling hypothesis applies to these examples with degenerate ground states, the quasicrystal should be entropically stable at finite T.

In summary the cluster picture incorporates the different predictions of previous models into a spectrum of cluster picture possibilities. At the same time, it suggests that quasicrystals may form under more robust conditions. Beginning from Penrose tilings, we find that matching rules can
ordered quasicrystalline structures are obtained. Beginning from maximally random tilings, the degeneracy of the ground state can be broken without forcing the system away from quasicrystallinity. Another implication of the cluster picture is quasicrystals should typically exhibit atomic structures with a much higher degree of order, less diffuse scattering (in diffraction experiments), and larger phason elastic constants compared to binary or maximally random tiling models. We are presently extending our calculations to 3D models with icosahedral symmetry (using clusters of fat and skinny rhombohedra [10]) for which the preliminary results seem similar. In 3D, the random tiling and cluster picture models result in Bragg rather than power-law peaks, but the degree of diffuse scattering is typically much lower in the cluster picture models. Our hope is that the cluster picture can unify the theoretical insights of prior models into an effective, natural explanation of observed quasicrystal properties.

We thank D. P. DiVincenzo, C. Henley, K. Ingersent, and J. E. S. Socolar for their critical reading of the manuscript, and especially F. Gähler for pointing out errors in an earlier version. This research was supported by the DOE at Penn (DOE-EY-76-C-02-3071).

[1] D. Shechtman, I. Blech, D. Gratias, and J. W. Cahn, Phys. Rev. Lett. **53**, 1951 (1984).
[2] Cf., H. Jónsson and H. C. Anderson, Phys. Rev. Lett. **60**, 2295 (1988).
[3] C. L. Henley, *Quasicrystals, The State of Art*, edited by D. P. DiVincenzo and P. J. Steinhardt (World Scientific, Singapore, 1991), pp. 429–524.
[4] S. Burkov, J. Phys. **2**, 695 (1992); Phys. Rev. Lett. **67**, 614 (1991).
[5] W. Steurer *et al.*, Acta Cryst. B **49**, 661 (1993).
[6] D. P. DiVincenzo, W. Krakow, P. A. Bancel, E. Cockayne, and V. Elser, J. Non-Cryst. Solids **153&154**, 145 (1993).
[7] L. Pauling, Nature (London) **317**, 512 (1985); Phys. Rev. Lett. **58**, 365 (1987).
[8] M. Boudard *et al.*, J. Phys. Condens. Matter **4**, 10 149 (1992).
[9] C. Janot and M. de Boissieu, Phys. Rev. Lett. **72**, 1674 (1994).
[10] D. Levine and P. J. Steinhardt, Phys. Rev. Lett. **53**, 2477 (1984); Phys. Rev. B **34**, 596 (1986).
[11] R. Penrose, Bull. Inst. Math. Its Appl. **10**, 266 (1974).
[12] L. S. Levitov, Commun. Math. Phys. **119**, 627 (1988); J. E. S. Socolar, Commun. Math.Phys. **129**, 599 (1990).
[13] L.-H. Tang and M. V. Jaric, Phys. Rev. B **41**, 4524 (1990); M. Widom, in *Quasicrystals*, edited by M. V. Jaric and S. Lundquist (World Scientific, Singapore, 1990), p. 337.
[14] H.-C. Jeong and P. J. Steinhardt, Phys. Rev. B **48**, 9394 (1993).
[15] J. Lee, Phys. Rev. Lett. **71**, 211 (1993).
[16] V. Elser, Phys. Rev. Lett. **54**, 1730 (1985).
[17] P. A. Kalugin, Pis'ma Zh. Eksp. Teor. Fiz. **49**, 406 (1989) [JETP Lett. **49**, 467 (1989)].
[18] N. de Bruijn, K. Nederl. Akad. Wetensch. Proc. Ser. A **84**, 1 (1981).
[19] V. Elser, Acta Cryst. Sect. A **42**, 36 (1986).
[20] A. Katz and M. Duneau, J. Phys. **47**, 181 (1986).
[21] T. C. Lubensky *et al.*, Phys. Rev. Lett. **57**, 1440 (1986).
[22] J. E. S. Socolar, T. C. Lubensky, and P. J. Steinhardt, Phys. Rev. B **34**, 3345 (1986).
[23] For values of Δx where $\alpha_2 \neq 0$, $\mathcal{U}(x)$ is concave such that, by the usual Gibbs construction, it is favorable to phase separate into domains of quasicrystal phase (plus some other phase).

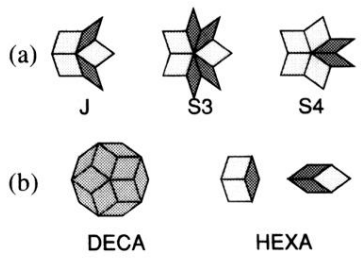

FIG. 1. Low-energy clusters selected for the examples in this paper: (a) C_P: J, $S3$, and $S4$; C_W: J and $S3$. (b) $C_{B/T}$: Decagon clusters (only the "star" decagon cluster is shown here, but there are five others) and the two hexagon clusters. C_D: star decagon cluster only.